

Dynamics of the Immune Reaction to Pancreatic Cancer from Inception to Invasion

Carolyn E. Clark,¹ Sunil R. Hingorani,^{3,4} Rosemarie Mick,² Chelsea Combs,¹ David A. Tuveson,¹ and Robert H. Vonderheide¹

¹Abramson Family Cancer Research Institute and ²Department of Biostatistics and Epidemiology, University of Pennsylvania School of Medicine, Philadelphia, Pennsylvania and ³Clinical Research and Public Health Sciences Divisions, Fred Hutchinson Cancer Research Center; ⁴University of Washington School of Medicine, Seattle, Washington

Abstract

The dynamics of cancer immunosurveillance remain incompletely understood, hampering efforts to develop immunotherapy of cancer. We evaluated the evolving *in vivo* immune response to a spontaneous tumor in a genetically defined mouse model of pancreatic ductal adenocarcinoma from the inception of preinvasive disease to invasive cancer. We observed a prominent leukocytic infiltration even around the lowest grade preinvasive lesions, but immunosuppressive cells, including tumor-associated macrophages, myeloid-derived suppressor cells (MDSC), and regulatory T cells (T_{reg}), dominated the early response and persisted through invasive cancer. Effector T cells, however, were scarce in preinvasive lesions, found in only a subset of advanced cancers, and showed no evidence of activation. The lack of tumor-infiltrating effector T cells strongly correlated with the presence of intratumoral MDSC with a near mutual exclusion. *In vitro*, we found that MDSC suppressed T-cell proliferation. Overall, our results show that suppressive cells of the host immune system appear early during pancreatic tumorigenesis, preceding and outweighing antitumor cellular immunity, and likely contribute to disease progression. Thus, in contrast to the hypothesis that an early “elimination phase” of cancer immunosurveillance is eventually overwhelmed by a growing invasive tumor, our findings suggest that productive tumor immunity may be undermined from the start. Efforts to test potent inhibitors of MDSC, tumor-associated macrophages, and T_{reg}, particularly early in the disease represent important next steps for developing novel immunotherapy of cancer. [Cancer Res 2007;67(19):9518–27]

Introduction

Tumorigenesis is initiated by genetic events and subsequently fueled and sculpted by additional pressures within the tumor microenvironment, including both the innate and the adaptive arms of the host immune system (1). Tumor cells express antigens as a result of genomic instability and aberrant gene expression, making them immunologically distinct from normal cells and, therefore, potential targets of host lymphocytes (2). Indeed, the

protective role of the immune system as a cellular mechanism of tumor suppression has been postulated for >50 years (3) and supported more recently by studies in immunodeficient mice (4–7). Clinical observations corroborate these findings: tumor-infiltrating lymphocytes, for example, have been associated with improved survival of patients with melanoma, as well as prostate, breast, colorectal, ovarian, and other carcinomas (8–13).

Not all immune cell types have tumor-suppressive potential, and thus, the immune system represents a double-edged sword. Tumor-promoting roles have been attributed to a number of immunocytes, including tumor-associated macrophages (14), myeloid-derived suppressor cells (MDSC; refs. 15–18), and even B cells (19). Furthermore, the chronic inflammatory state of the tumor microenvironment can promote genomic damage and can foster recruitment of immunosuppressive cell populations, such as regulatory T cells (T_{reg}), that dampen antitumor immune responses (20, 21).

Dynamic cellular interactions of immunocytes responding to a foreign antigen have been well characterized and directly visualized in elegant studies (22, 23), and although theories abound regarding the naturally occurring *in vivo* immune responses to tumor cells during the course of disease progression, these responses have never been studied directly. Mouse models using implanted syngeneic or xenogeneic tumors do not provide information about the early stages of neoplastic progression nor do they recapitulate the native microenvironment of an endogenously growing tumor. Moreover, dynamic studies of the interactions of immune cells with preinvasive and invasive human tumors are necessarily limited by tissue availability. With increasingly sophisticated genetic engineering techniques allowing for a new generation of mouse models of cancer, it has recently become possible to study, in a physiologically relevant system, the dynamic and complex interplay between tumor and immune system as it evolves with disease progression.

We have recently described a mouse model of preinvasive and invasive pancreatic ductal adenocarcinoma (PDA) that faithfully recapitulates the salient clinical, histopathologic, and molecular features of the human disease (24, 25). In this model, an endogenous *Kras* allele is targeted to carry an activating mutation in codon 12, preceded by a floxed transcriptional and translational silencing cassette in the promoter region rendering the allele quiescent. Conditional expression of the *Lox-STOP-Lox-Kras*^{G12D} allele is achieved by breeding these animals with mice expressing *Cre* recombinase, driven by the pancreatic-specific promoters *Pdx-1* or *p48*, resulting in tissue-restricted excision of the “STOP” cassette and transcription of the oncogenic *Kras*^{G12D} allele. Endogenous expression of this activated *Kras* allele is sufficient to initiate pancreatic intraepithelial neoplasias (PanIN) that progress through all the histologic stages described for the human disease (26). These

Note: Supplementary data for this article are available at Cancer Research Online (<http://cancerres.aacrjournals.org/>).

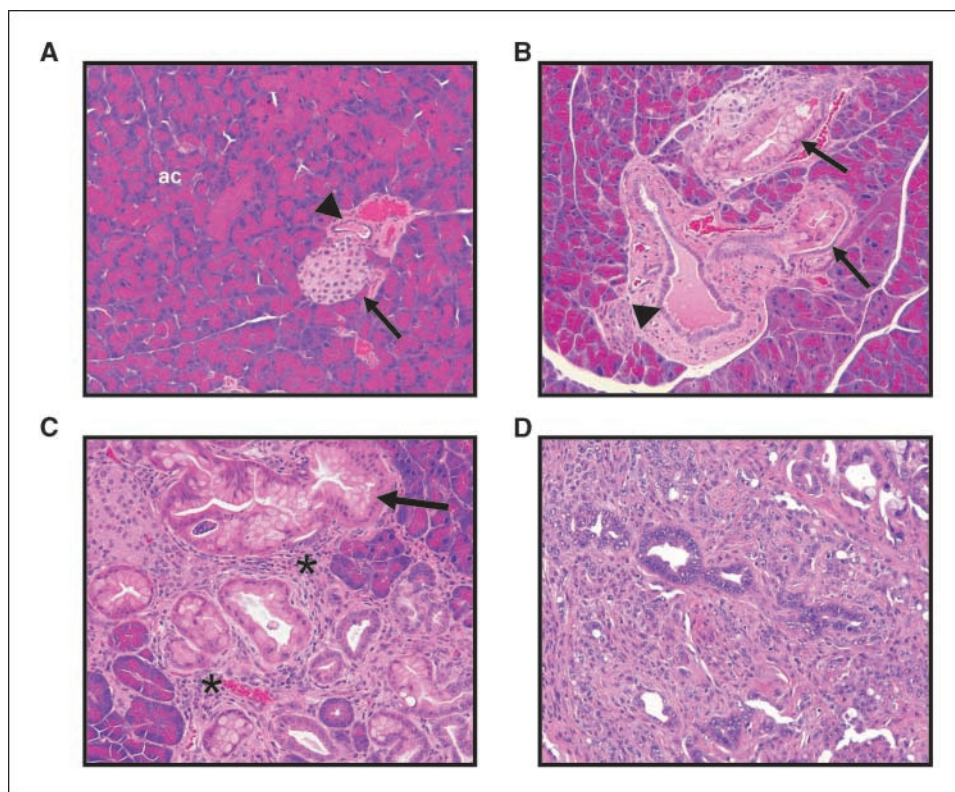
R.H. Vonderheide and S.R. Hingorani contributed equally to this work.

Requests for reprints: Robert H. Vonderheide, 421 Curie Boulevard, 551 BRB II/III, Philadelphia, PA 19104. Phone: 215-573-4265; Fax: 215-573-2652; E-mail: rhv@mail.med.upenn.edu or Sunil R. Hingorani, 1100 Fairview Avenue N, M5-C804, Seattle, WA 98109. Phone: 206-667-7763; E-mail: srh@fhcrc.org.

©2007 American Association for Cancer Research.

doi:10.1158/0008-5472.CAN-07-0175

Figure 1. Progression of pancreatic neoplasia in *Kras*^{G12D} mice is accompanied by a fibroinflammatory reaction composed of leukocytes and stromal elements. **A**, normal pancreas with abundant acinar tissue (*ac*) around an islet (*arrow*) and adjacent normal duct (*arrowhead*). **B**, early stage PanIN lesions (*arrows*) and adjacent normal duct seen in tangential section (*arrowhead*). Note the developing stroma surrounding ductal structures. **C**, Higher-grade PanIN lesions (*arrow*) with an increasingly robust fibroinflammatory response (*asterisks*). **D**, infiltrating PDA with abundant desmoplasia. Magnification for all images are 200 \times .



lesions ultimately culminate in invasive and metastatic PDA through the stochastic acquisition of additional mutations (24).

The emergence of an intense fibroinflammatory reaction, composed of stromal and immune cells, accompanies the progression from normal histology to PDA in human pancreatic cancer and is also recapitulated in *Kras*^{G12D} mice. Indeed, this robust desmoplastic response is an invariant and virtually pathognomonic feature of the malignant state, suggesting a potentially important role in disease evolution. Here, we characterize the components and dynamics of the immune response in *Kras*^{G12D} mice as a function of pancreatic tumor progression.

Materials and Methods

Mouse strains. Mice endogenously expressing a single mutant *Kras* allele in progenitor cells of the pancreas were generated as previously described (24). Briefly, *Lox-STOP-Lox (LSL)-Kras*^{G12D} mice were bred with *Pdx-1-Cre* or *p48*^{Cre} mice that express *Cre* recombinase from pancreatic-specific promoters. All procedures were done in accordance with IACUC guidelines of the University of Pennsylvania.

Histology and immunohistochemistry. Histology was examined by H&E staining of 6- μ m sections of formalin-fixed, paraffin-embedded tissue. Immunohistochemical stains were done on 9- μ m sections of frozen tissue. When necessary, endogenous peroxidase activity was quenched with H₂O₂. Primary antibodies and the empirically determined dilutions used were CD45 (clone 30-F11, 1:50), CD4 (clone RM4-5, 1:40), CD8 (clone 53-6.7, 1:20), CD11b (clone M1/70, 1:40), and Gr-1 (clone RB6-8C5, 1:20; all from BD Biosciences Pharmingen). Biotin-conjugated goat anti-rat secondary antibody (BD Biosciences Pharmingen) was used at a dilution of 1:200. The Elite Vectastain ABC kit and peroxidase substrate 3,3'-diaminobenzidine kit (Vector Laboratories) were used for signal detection according to the manufacturer's recommendations. Sections were counterstained with hematoxylin. Photographs were taken with a Nikon ECLIPSE 50i

microscope and DXM1200F digital camera using ACT-1 software (all from Nikon).

Flow cytometry and cell sorting. Single-cell suspensions of fresh spleen, pancreas, and other tissues were prepared as follows: spleens were crushed and passed through a 70- μ m cell strainer, washed once with RPMI/10% FCS, and treated with ACK cell lysis buffer (Cambrex Bio Science) to eliminate RBC. Pancreata were minced using sterile scalpels, then incubated in 1 mg/mL collagenase (Sigma-Aldrich) in RPMI for 30 min at 37 $^{\circ}$ C before passing through a 70- μ m cell strainer. Single-cell suspensions were stained in PBS/2% FCS with the following antibodies: CD45 (clone 30-F11), CD3 ϵ (clone 145-2C11), CD4 (clone RM4-5), CD8 α (clone 53-6.7), CD25 (clone PC61), CD44 (clone IM7), CD45RB (clone 16A), CD62L (clone MEL-14), CD69 (clone H1.2F3), CD19 (clone 1D3), CD45R/B220 (clone RA3-6B2), CD49b (clone DX5), CD11b (clone M1/70), and Gr-1 (clone RB6-8C5; all from BD Biosciences Pharmingen). For intracellular staining of Foxp3, cells were permeabilized and stained with the APC anti-mouse/rat Foxp3 staining set (eBioscience) according to the manufacturer's recommendations. Flow cytometry was done using a BD FACSCanto (BD Biosciences Immunocytometry Systems), and data were analyzed with BD FACSDiva software. Cells were sorted with a MoFlo high-performance cell sorter (DakoCytomation) using Summit v4 software.

Cellular proliferation assays. T_{reg} suppression assays were done in triplicate in 96-well, flat-bottom plates. Unfractionated splenocytes (1×10^5 /well) or sorted CD4⁺ CD25⁻ T cells (5×10^4 /well) were stimulated with CD3 or CD3 and CD28 antibodies (each at 1 μ g/mL). Sorted autologous CD4⁺ CD25⁺ T cells were added at various ratios. [³H]thymidine (1 μ Ci/well; Perkin-Elmer) was added on day 3, and plates were harvested 18 h later onto glass fiber filters (Wallac Oy) using a Tomtec harvester (Tomtec). Filters were sealed in sample bags (Wallac Oy) with 4 mL scintillation fluid, and counts were measured on a 1450 Microbeta Trilux (Wallac Oy).

MDSC suppression assays were done in triplicate in 96-well, flat-bottom plates. Sorted splenic T cells (5×10^4 /well) were stimulated with either 5 μ g/mL concanavalin A (ConA; Sigma-Aldrich) or plate-bound CD3 antibody (BD Discovery Labware). Sorted autologous Gr1⁺ CD11b⁺ cells were irradiated at 60 Gy before plating (5×10^3 /well) with the responder

T cells. [^3H]thymidine (1 $\mu\text{Ci}/\text{well}$) was added on day 3, and plates were harvested 18 h later as described above.

Quantitative PCR. $\text{CD4}^+ \text{CD25}^+$ and $\text{CD4}^+ \text{CD25}^-$ T cells or B220^+ B cells were sorted from either spleen or tumor, and RNA was extracted using the RNeasy Micro kit (QIAGEN). cDNA was prepared using the Superscript first-strand synthesis kit (Invitrogen). Quantitative PCR was done for Foxp3 using the following primers: F: 5'-CCAGGAAAGACAGCAACCTT-3'; R: 5'-TTCTCACAACCAGGCCACTTG-3'. A custom FAM dye/MGB probe for Foxp3 was obtained from Applied Biosystems with the following sequence: 6FAM ATCCTACCCACTGCTGGCAAAATGGAGT CMGBNFQ. Primers and FAM dye/MGB probes for mouse β -actin and eukaryotic 18S rRNA were purchased as predeveloped TaqMan assay reagents (Applied Biosystems) for use as internal controls. PCR reactions were run in MicroAmp optical 96-well reaction plates on a 7900HT fast real-time PCR system (Applied Biosystems).

Statistical analyses. All statistical analyses were done with SPSS 12.0 software (SPSS, Inc.). Distributions of continuous variables were described by means and SEs. The null hypothesis that mean values were equal among three groups (e.g., normal, PanIN, and PDA) versus the alternative hypothesis that mean values were not all equal was tested by ANOVA, with post-hoc paired comparisons tested by the Scheffe test. The correlations between myeloid cell populations and T-cell populations among total CD45^+ cells were modeled by both linear and nonlinear

(exponential) regression. In all cases, these correlations were best fit by an exponential model, $y = \beta_0 e^{\beta_1 x}$, wherein β_0 is the intercept and β_1 is the slope. The null hypothesis of no correlation ($\beta_1 = 0$) was determined by a Wald test. The coefficient of determination, R^2 , indicated the percentage of total variation in y (myeloid cells) that was explained by x (T-cell populations). For all tests, a P value of ≤ 0.05 was considered statistically significant.

Results

Influx of leukocytes during progression of pancreatic neoplasia. $LSL\text{-}Kras^{G12D/+};Pdx\text{-}1\text{-}Cre$ mice and $LSL\text{-}Kras^{G12D/+};p48^{Cre}$ mice (referred to here collectively as $Kras^{G12D}$ mice) develop preinvasive PanINs as early as 2 weeks of age with complete penetrance (24, 27). Both the number and grade of PanIN lesions increase with age, and the mice ultimately develop invasive PDA, frequently accompanied by metastases to the lung, liver, and elsewhere. Disease progression in the pancreas of $Kras^{G12D}$ mice was accompanied by a gradual replacement of acinar parenchyma with a stromal reaction consisting of leukocytes, fibroblasts, and collagen deposition, as clearly discerned on H&E stains (Fig. 1). In mice with PDA, this reaction strongly resembled the desmoplasia

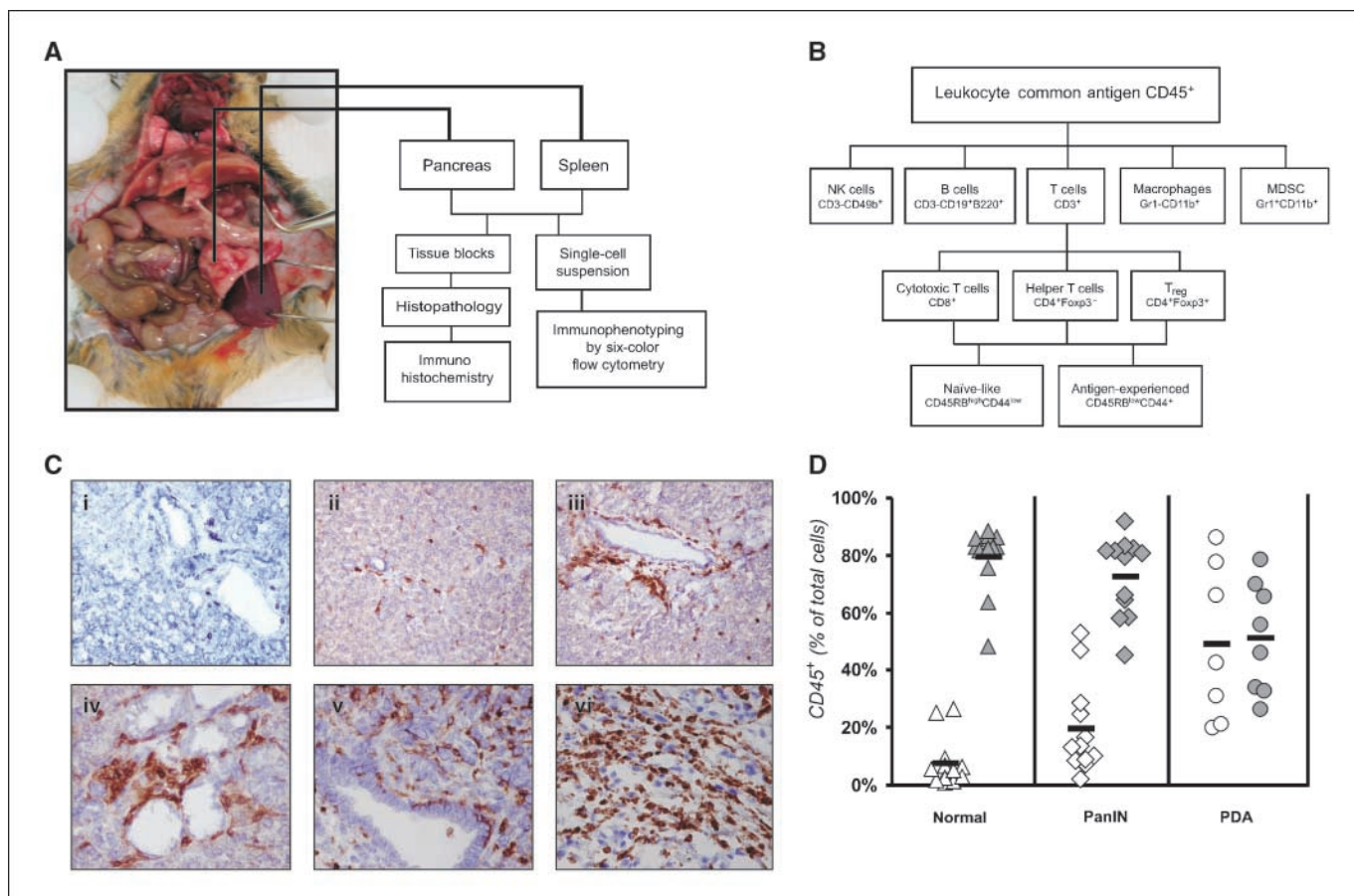
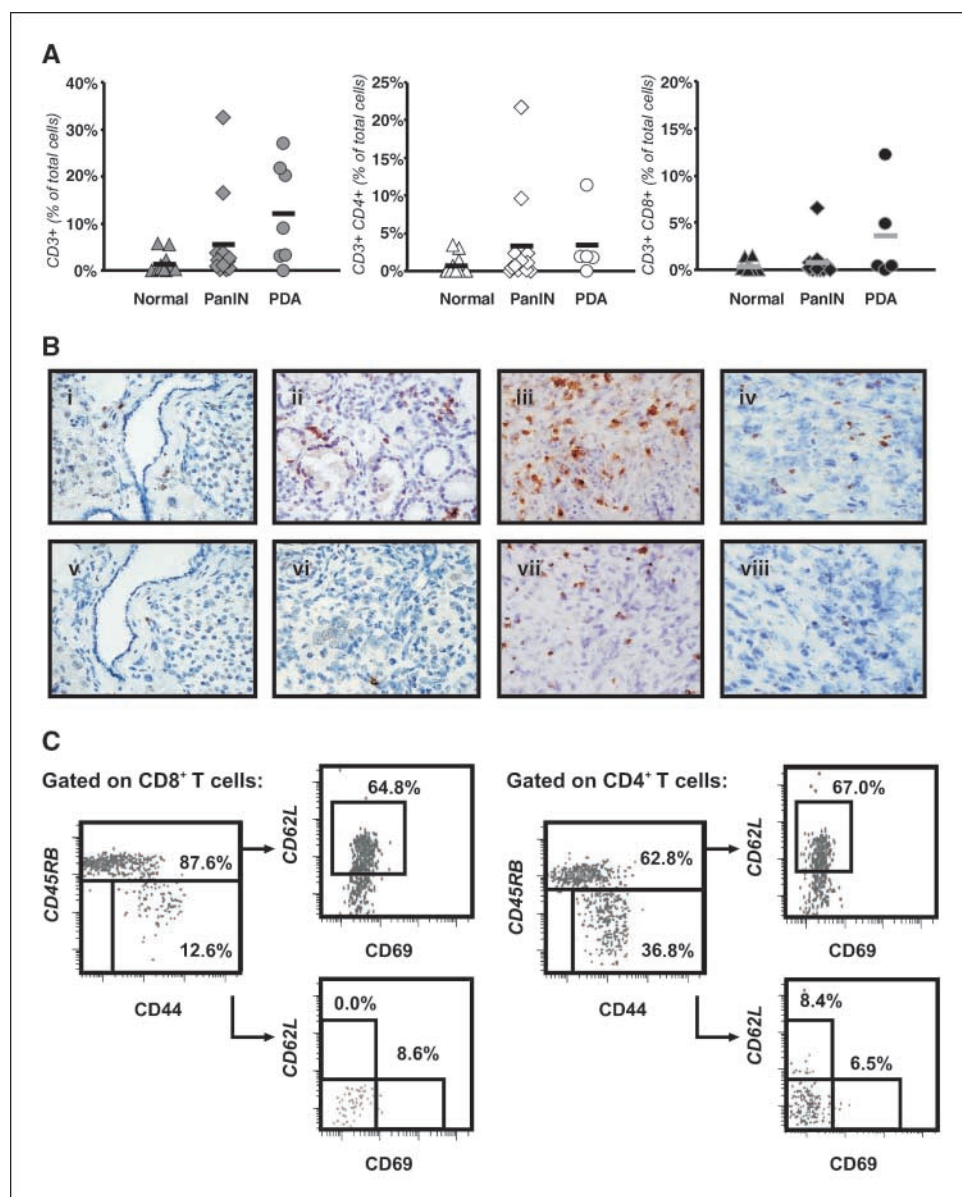


Figure 2. Characterization of leukocytic infiltrates in pancreata of normal, PanIN, and PDA mice. *A*, from each mouse, the pancreatic tumor (or the head of the pancreas in the absence of a tumor) was harvested along with the spleen and other organs. A portion of tissue was preserved for histopathology and immunohistochemistry, and the remainder was prepared as a single-cell suspension for analysis by flow cytometry. *B*, flow cytometric approach to identify leukocyte subsets defined by characteristic cell-surface molecular phenotypes. *C*, immunohistochemical detection of CD45 expression in normal pancreas (*i*), normal region of PanIN pancreas (*ii*), neoplastic regions of PanIN pancreas (*iii* and *iv*), pancreatic tumor and duct in PDA pancreas (*v*), desmoplastic region in PDA pancreas (*vi*). Original magnification, 200 \times (*i-iii*) and 400 \times (*iv-vi*). *D*, mean percentage of CD45⁺ cells in the pancreas (white symbols) and spleen (gray symbols) were statistically different among normal (triangles; $n = 13$), PanIN (diamonds; $n = 12$), and PDA (circles; $n = 8$) mice as determined by flow cytometry ($P < 0.001$ by three-way ANOVA). Symbols, data from each animal; black bars, mean percentage for the group. Details of the statistical analysis including mean and SE are noted in Supplementary Tables S1 and S2.

Figure 3. Characterization of T cells in pancreas of normal, PanIN, and PDA mice. **A**, percentage of T-cell subsets in the pancreas from normal (triangles; $n = 13$), PanIN (diamonds; $n = 12$), and PDA (circles; $n = 7$) mice as determined by flow cytometry. *Left*, total CD3⁺ T cells; *middle*, CD3⁺ CD4⁺ T cells; *right*, CD3⁺ CD8⁺ T cells. Comparison of means by three-way ANOVA: $P = 0.02$ for CD3⁺ T cells, $P = 0.29$ for CD4⁺ T cells, and $P = 0.04$ for CD8⁺ T cells. Symbols, data from each animal; bars, mean percentage for the group. **B**, immunohistochemical detection of CD4 in normal pancreas (i), PanIN pancreas (ii), two different PDA pancreata (iii and iv), and of CD8 in normal pancreas (v), PanIN pancreas (vi), and two different PDA pancreata (vii and viii). *iii–iv* and *vii–viii*, variability in T-cell infiltration between animals. Original magnification, 400 \times (i–ii and v–vi) and 200 \times (iii–iv and vii–viii). **C**, after gating on CD45⁺ CD3⁺ CD8⁺ lymphocytes (left) or CD45⁺ CD3⁺ CD4⁺ lymphocytes (right), subsequent daughter gates were drawn to separate CD45RB^{high} CD44^{low} naive-like T cells from CD45RB^{low} CD44^{high} antigen-experienced T cells and then to examine CD62L and CD69 expression on each of these populations. Numbers, percentages of the parent gate. Representative flow cytometric results are shown for one of four PDA mice. Details of the statistical analysis including mean and SE are noted in Supplementary Table S1.



classically seen in human pancreatic cancer (28). To define the involvement of leukocytes as pancreatic tumorigenesis progresses, cohorts of *Kras*^{G12D} mice were sacrificed at defined time points between 3 and 10 months of age; an additional cohort was followed longitudinally until moribund of PDA. The pancreatic tumor or, in the absence of a tumor, the head of the pancreas, was harvested at necropsy. Spleen and bone marrow were also harvested, as well as the salivary gland, as a comparative exocrine gland (control). Portions of these tissues were processed in parallel for histopathologic examination and immunohistochemical studies, whereas the remainder was prepared into single-cell suspensions for analysis by multivariable flow cytometry (Fig. 2A). Tissues from normal littermates (i.e., those lacking the *Kras*^{G12D} allele, *Cre* recombinase, or both) served as controls. We note that although the overall number and grade of PanIN lesions progress over time, at any given point, multiple lesions spanning all grades are present. Thus, it is not possible to categorize animals as containing exclusively PanIN-1, PanIN-2, or PanIN-3 lesions. Instead, and most significantly, a

distinction is made between animals containing preinvasive versus invasive disease. Animals with preinvasive ductal lesions only are called PanIN mice here, whereas those demonstrating evidence of infiltrating ductal carcinomas are called PDA mice.

To determine the contribution of leukocytes in the stromal reaction, we characterized cells expressing the leukocyte common antigen (CD45) in pancreas and spleen both *in situ* by immunohistochemistry and *ex vivo* by flow cytometry (Fig. 2B). We found that the succession from normal histology to preinvasive PanIN to invasive PDA was accompanied by a progressive infiltration of CD45⁺ cells ($P < 0.001$ by ANOVA). The pancreata of control mice and the histologically normal areas of pancreata from PanIN mice contained few CD45⁺ cells (Fig. 2C). By flow cytometry, $7.5 \pm 2.6\%$ (mean \pm SE) of total cells from normal pancreas expressed CD45 (Fig. 2D). In contrast, we observed a prominent CD45⁺ cellular infiltrate in regions harboring preinvasive disease, with CD45⁺ leukocytes clustered preferentially around individual neoplastic ducts (Fig. 2C). By flow cytometry, $19.5 \pm 4.7\%$ of total cells from

pancreata of PanIN mice expressed CD45 (Fig. 2D). In PDA, the CD45⁺ infiltrate was even more intense, with CD45⁺ leukocytes intermixed with carcinoma cells and streams of CD45⁺ cells observed within the areas of dense fibrosis (Fig. 2C). Remarkably, CD45⁺ leukocytes comprise 49.3 ± 10.3% of total cells within the cell suspensions prepared from invasive pancreatic ductal carcinomas (Fig. 2D). This inflammatory reaction in the pancreatic carcinomas was accompanied by a decrease in the percentage of CD45⁺ cells in the spleen (*P* = 0.001). The spleens of animals with PDA were typically enlarged and exhibited evidence of extramedullary hematopoiesis, including nucleated RBC and megakaryocytes, likely contributing to the observed decrease in the percentage of CD45⁺ cells.

Absence of detectable effector T-cell response. To characterize further the composition of the CD45⁺ infiltrate in neoplastic pancreata, we next used multivariable flow cytometry, as well as immunohistochemistry, to examine leukocyte subsets defined by cell surface phenotypes. We focused first on the presence of tumor-infiltrating T cells (CD3⁺) in light of increasing evidence that their presence in human cancers is associated with improved clinical

outcomes (12, 13). Although CD3⁺ T cells were rare in normal pancreata, progression to PanIN and PDA was on average accompanied by a progressive infiltration of CD3⁺ T cells (*P* = 0.02; Fig. 3A, left). This effect was heterogeneous, however, with some mice exhibiting brisk T-cell infiltration and not others. In pancreata with PanIN lesions, the infiltrating T cells were primarily CD4⁺ T cells (Fig. 3A, middle), whereas CD8⁺ T cells were scarce (Fig. 3A, right). In PDA, infiltration with both CD4⁺ T cells and CD8⁺ T cells was observed, but only in a subset of mice. Immunohistochemistry corroborated these observations (Fig. 3B). In the spleen, the mean percentages of CD3⁺ T cells, CD4⁺ T cells, and CD8⁺ T cells among total splenocytes were comparable in both normal and PanIN mice, but in each case dropped significantly in mice with invasive carcinoma (*P* < 0.001 for each variable), likely related to the disruption of splenic architecture by extramedullary hematopoiesis (data not shown).

To determine if the intratumoral T cells exhibited evidence of activation and thus potentially contributed to productive antitumor immunity, we further analyzed these T cells for surface expression of CD45RB, CD44, CD62L, and CD69. Naive T cells express high levels of

Downloaded from http://aacrjournals.org/cancerres/article-pdf/67/19/9518/2572497/9518.pdf by guest on 14 June 2024

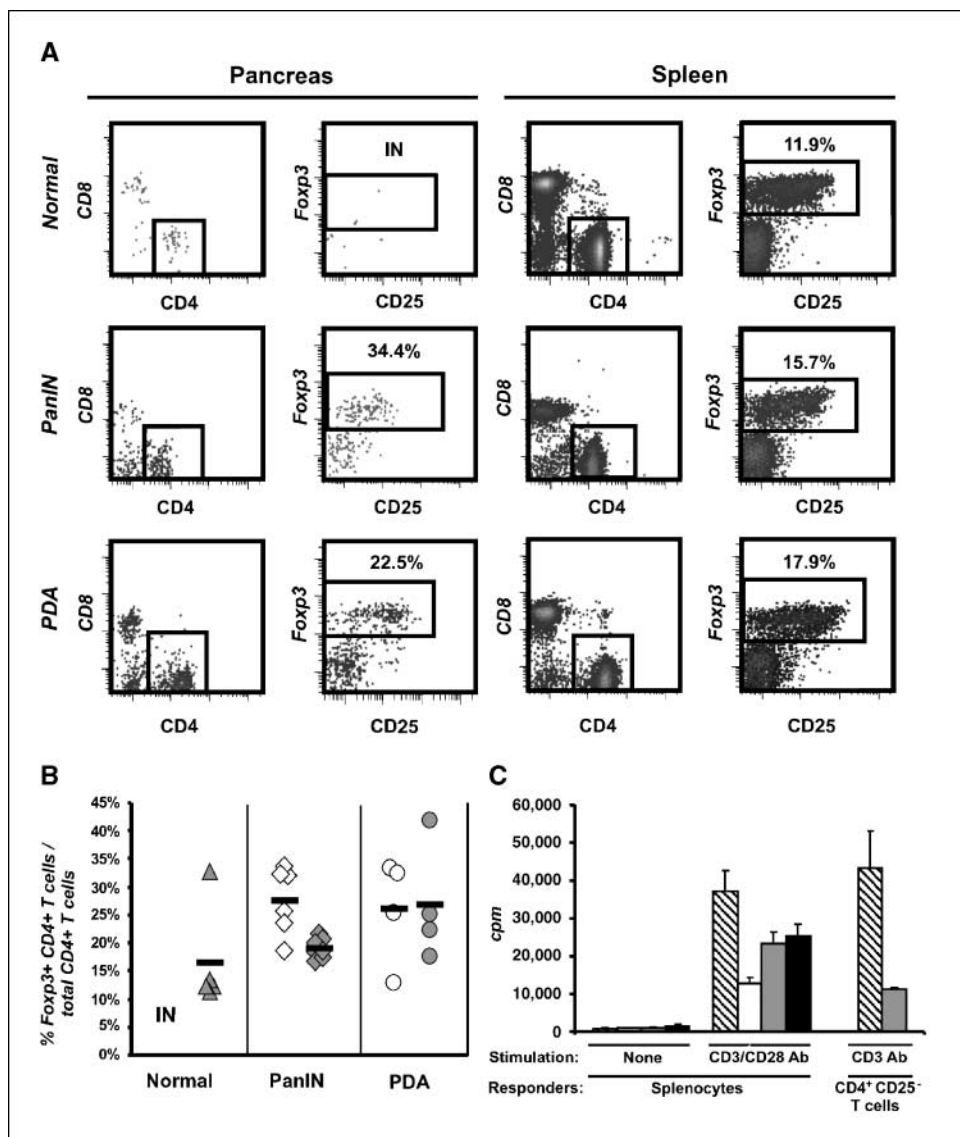


Figure 4. Characterization of CD4⁺ T_{reg} in pancreas and spleen of normal, PanIN, and PDA mice. **A**, flow cytometric results for pancreas or spleen from one representative mouse per group. After gating on CD45⁺ CD3⁺ T cells, cells were subsequently gated on CD4⁺ CD8⁻ T cells (first and third columns) to examine intracellular Foxp3 versus surface CD25 staining (second and fourth columns). Numbers, percentages of CD4⁺ Foxp3⁺ T cells among total CD4⁺ T cells; IN, insufficient number of events for accurate determination of percentage. **B**, percentage of CD4⁺ Foxp3⁺ T cells among total CD4⁺ T cells in the pancreas (white symbols) and spleen (gray symbols) from normal (triangles; *n* = 5), PanIN (diamonds; *n* = 7), and PDA (circles; *n* = 4) mice as determined by flow cytometry. Symbols, data from each animal; black bars, mean percentage for the group. Details of the statistical analysis including mean and SE are noted in Supplementary Tables S1 and S2. **C**, proliferation, measured by [³H]thymidine incorporation, of splenocytes or purified CD4⁺ CD25⁻ splenic T cells in media alone or in response to antibody stimulation, in the absence of autologous CD4⁺ CD25⁺ T cells (hatched columns) or in the presence of autologous CD4⁺ CD25⁺ T cells at suppressor/responder ratios of 1:4 (white columns), 1:8 (gray columns), and 1:20 (black columns). Bars, SD. *P* < 0.002 for differences between responder cells with versus without the addition of CD4⁺ CD25⁺ T cells (Student's *t* test). Data from two different mice, representative of five independent experiments.

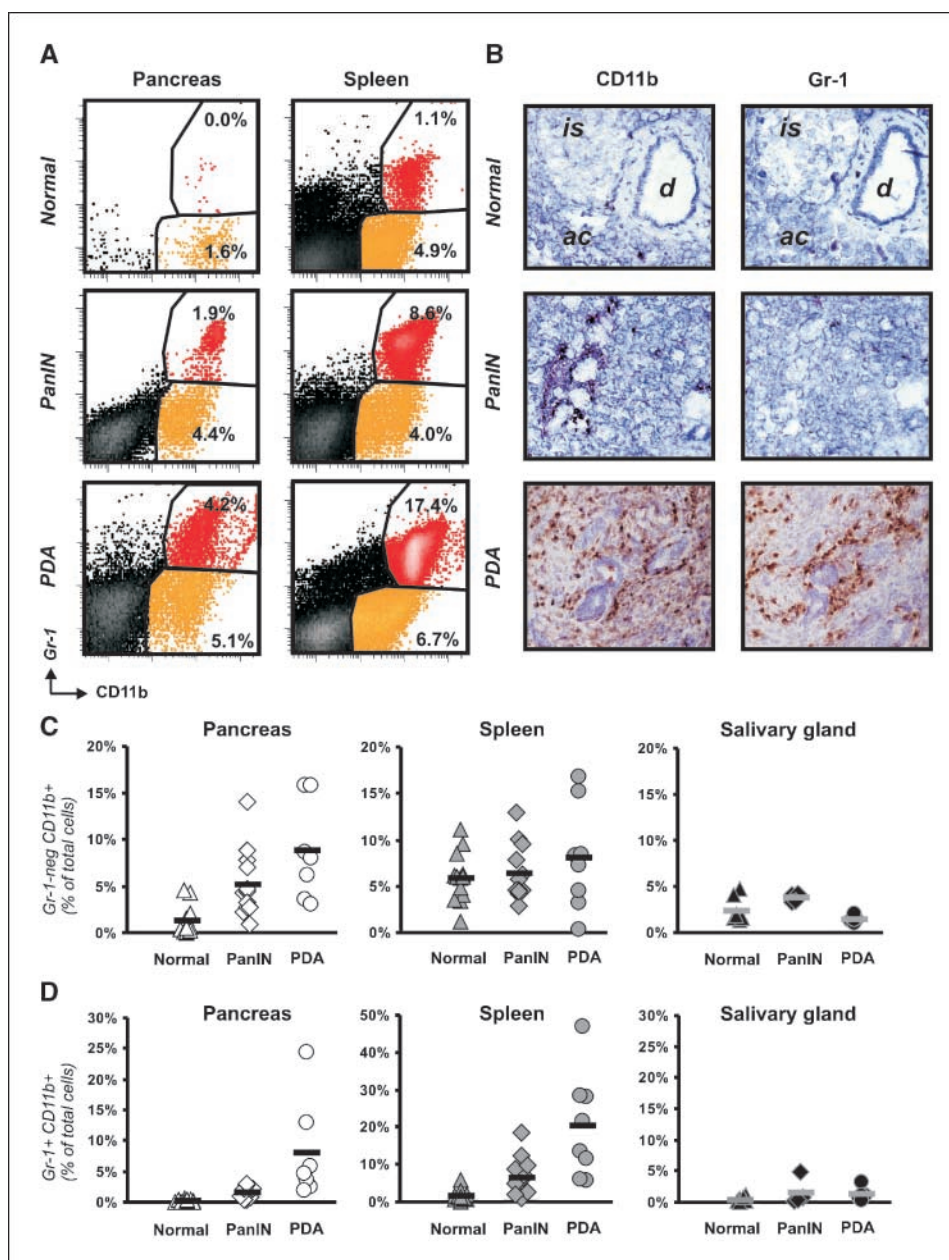


Figure 5. Characterization of myeloid cells in pancreas and spleen of normal, PanIN, and PDA mice. *A*, representative flow cytometric results for one mouse from each group. Cells were gated for CD45 expression and then analyzed for CD11b versus Gr-1 expression. Numbers, percentages of Gr-1⁺ CD11b⁺ MDSC or Gr-1⁻ CD11b⁺ macrophages among total cells. *B*, immunohistochemical detection of CD11b and Gr-1 expression in serial sections of normal pancreas (top), PanIN pancreas (middle), and PDA pancreas (bottom). Original magnification, 200 \times . *C*, mean percentages of Gr-1⁻ CD11b⁺ macrophages among total cells in the pancreas (left) were statistically significantly different among normal (triangles; $n = 13$), PanIN (diamonds; $n = 12$), and PDA (circles; $n = 8$) mice as determined by flow cytometry ($P < 0.001$). Post-hoc testing by the Scheffe test revealed that the increase in macrophages was significant between normal and PanIN pancreata ($P = 0.03$) rather than between PanIN and PDA pancreata ($P = 0.12$). Mean percentages of Gr-1⁻ CD11b⁺ macrophages among total cells in the spleen (middle) were not statistically different among normal (triangles; $n = 13$), PanIN (diamonds; $n = 12$), and PDA (circles; $n = 8$) mice ($P = 0.43$). There was also no statistically significant increase in the mean percentage of Gr-1⁻ CD11b⁺ macrophages among total cells in the salivary gland (right). Symbols, data from each animal; bars, mean percentage for the group. *D*, mean percentages of Gr-1⁺ CD11b⁺ MDSC among total cells in the pancreas (left) and spleen (middle) were statistically significantly different among normal (triangles; $n = 13$), PanIN (diamonds; $n = 12$), and PDA (circles; $n = 8$) mice as determined by flow cytometry ($P < 0.001$ for pancreas and $P < 0.001$ for spleen). Post-hoc testing by the Scheffe test revealed that the increase in MDSC was significant between PanIN and PDA pancreata ($P = 0.004$) rather than between normal and PanIN pancreata ($P = 0.65$). Post-hoc testing by the Scheffe test revealed that the increase in MDSC in the spleen was significant between PanIN and PDA ($P = 0.001$) rather than between normal and PanIN ($P = 0.30$). Mean percentages of Gr-1⁺ CD11b⁺ MDSC among total cells in the salivary gland (right) were not statistically different among normal (triangles; $n = 9$), PanIN (diamonds; $n = 4$), and PDA (circles; $n = 5$) mice as determined by flow cytometry ($P = 0.23$). Symbols, data from each animal; bars, mean percentage for the group. Details of the statistical analysis, including mean and SE, are noted in Supplementary Tables S1 and S2.

CD45RB and low levels of CD44, whereas antigen-experienced T cells, including activated T cells, T_{reg}, and memory T cells, are CD45RB^{low} and CD44^{high} (29). CD62L, expressed on naive T cells, is rapidly lost upon activation and reexpressed when the cells

differentiate into memory T cells. Activation of either naive or memory subsets is also marked by induction of CD69. More than 85% of intratumoral CD8⁺ T cells from PDA mice were CD45RB^{high} CD44^{low}, and among these, most cells were CD62L⁺ and CD69⁻

(Fig. 3C). Most of the intratumoral CD4⁺ T cells displayed a similar phenotype, but about one-third of CD4⁺ T cells in PDA showed evidence of antigen experience (CD45RB^{low} CD44^{high}). However, these cells were nearly all CD62L⁻ and CD69⁻ (Fig. 3C), inconsistent with an activated or memory phenotype. Although phenotypic markers cannot conclusively determine if infiltrating T cells are truly naive or functionally inactivated, there was nevertheless no significant immunophenotypic evidence of an ongoing effective immune response in these tumors.

Influx of T_{reg} early in disease progression. Given the absence of effector T cells in pancreatic neoplastic lesions in *Kras*^{G12D} mice, we investigated the contribution of immunosuppressive leukocytes during pancreatic cancer progression. One such cell type, T_{reg}, represents a population of CD4⁺ T cells that inhibits cellular immune responses and has been implicated in hindering antitumor immunity (30, 31). Based on intracellular staining for Foxp3, a transcription factor that defines T_{reg} (32–34), we found that 27.7 ±

2.4% (mean ± SE) of the total CD4⁺ T cells in PanIN and 26.1 ± 4.7% of the total CD4⁺ T cells in PDA pancreata were Foxp3⁺ (Fig. 4A and B). As expected, CD4⁺ Foxp3⁺ T cells were CD45RB^{low} CD44^{high} (data not shown). CD8⁺ T cells, on the other hand, were Foxp3⁻, also as expected (data not shown). Thus, compared with normal pancreata, in which CD4⁺ Foxp3⁺ T cells were too few to characterize, these findings reveal a marked infiltration of T_{reg} into the pancreas even before the development of invasive disease. In the spleen, CD4⁺ Foxp3⁺ T_{reg} were evident not only in preparations from mice with PanIN or PDA, but also from normal mice (Fig. 4A and B).

Expression of the interleukin 2 (IL-2) receptor α chain CD25 has also been used to identify T_{reg}, albeit with lower sensitivity and specificity than Foxp3 (35, 36). We found that most but not all CD4⁺ Foxp3⁺ T_{reg} express CD25, both in the pancreas and spleen regardless of histopathology (Fig. 4A). Purified CD4⁺ CD25⁺ T cells from PDA pancreas or spleen expressed Foxp3 mRNA by

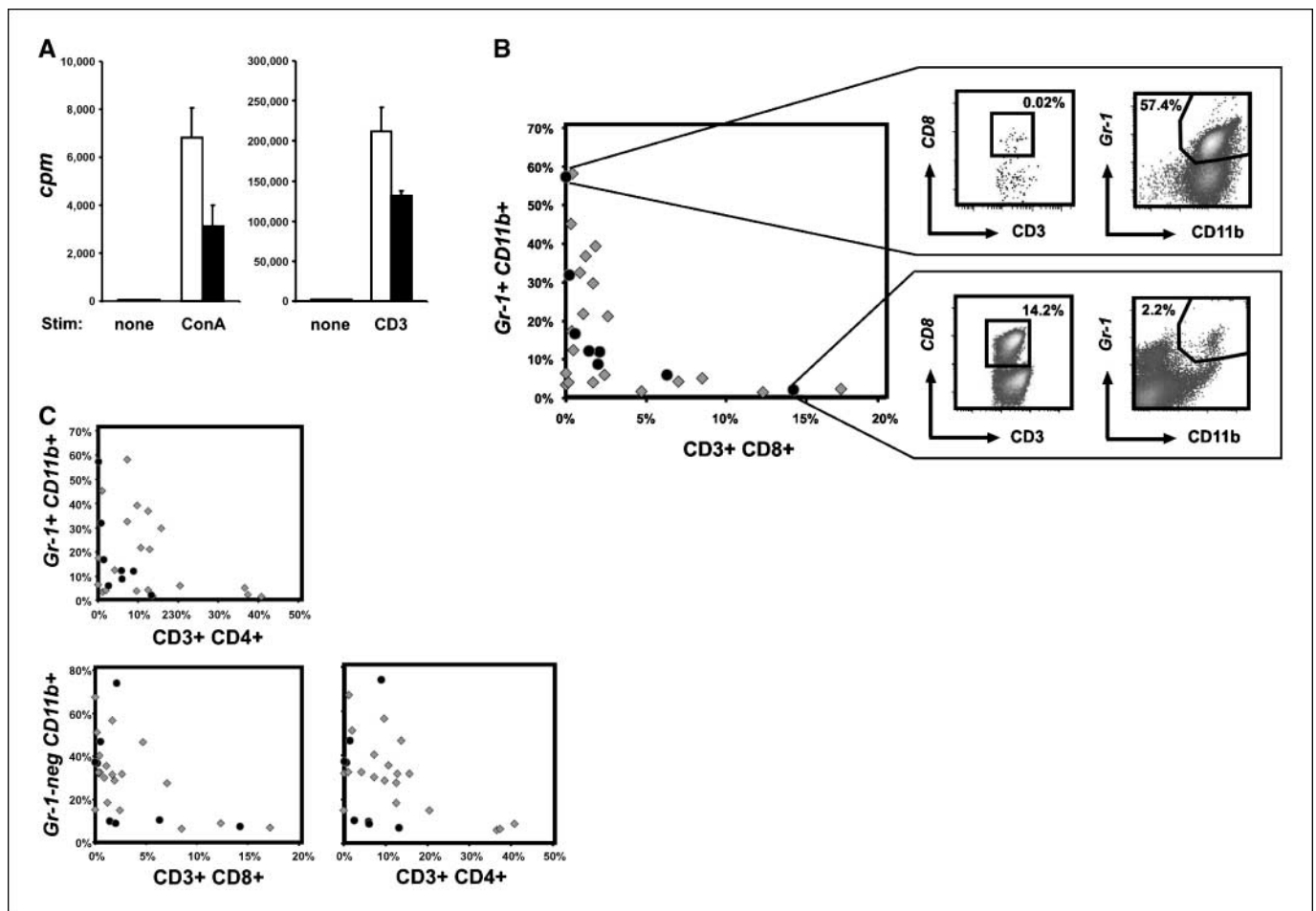


Figure 6. Function of MDSC and *in vivo* relationships between myeloid and T-cell populations among CD45⁺ leukocytes in the diseased pancreas. **A**, proliferation, measured by [³H]-Thymidine incorporation, of sorted splenic T cells with media alone or with mitogenic stimulation (ConA; left) or antibody stimulation (CD3; right). Proliferation of stimulated T cells alone (white columns) is significantly diminished ($P < 0.02$, Student's *t* test) when irradiated Gr1⁺ CD11b⁺ MDSC are added at an MDSC/T cell ratio of 1:10 (black columns). Bars, SD. **B**, near mutual exclusion between Gr-1⁺ CD11b⁺ MDSC and CD3⁺ CD8⁺ T cells among CD45⁺ cells in the pancreata of PanIN and PDA mice. Gray diamonds, PanIN mice ($n = 20$); black circles, PDA mice ($n = 8$). These data were best fit by an exponential model, with slope of -0.155 ($P = 0.0002$) and coefficient of determination (R^2) of 0.413, indicating that 41% of the variation in Gr-1⁺ CD11b⁺ values were explained by CD3⁺ CD8⁺. Flow cytometry plots of Gr-1⁺ CD11b⁺ MDSC and CD3⁺ CD8⁺ T cells from two PDA mice show the opposite extremes of the spectrum. Left flow cytometry plots are first gated on CD45⁺ CD3⁺ T cells; right flow cytometry plots are first gated on CD45. Numbers, percentages of total CD45⁺ cells. **C**, top, relationship between Gr1⁺ CD11b⁺ MDSC and CD3⁺ CD4⁺ T cells among CD45⁺ cells in the pancreata of PanIN and PDA mice. Gray diamonds, PanIN mice ($n = 20$); black circles, PDA mice ($n = 8$). Exponential slope = -0.047 ($P = 0.011$); $R^2 = 0.223$. Bottom, relationships between Gr1⁻ CD11b⁺ macrophages and CD3⁺ CD8⁺ T cells (left) or Gr1⁻ CD11b⁺ macrophages and CD3⁺ CD4⁺ T cells (right) among CD45⁺ cells in the pancreata of PanIN and PDA mice. Gray diamonds, PanIN mice ($n = 20$); black circles, PDA mice ($n = 8$). CD8⁺ T cells: exponential slope = -0.109 ($P = 0.0001$), $R^2 = 0.460$; CD4⁺ T cells: exponential slope = -0.037 ($P = 0.0015$), $R^2 = 0.325$.

quantitative PCR, whereas purified splenic B cells from the same animals did not (data not shown).

We tested the suppressive function of CD4⁺ CD25⁺ T cells in this model in standard mixed lymphocyte reactions measuring [³H]thymidine incorporation to quantify cell proliferation. Bulk splenocytes or sorted CD4⁺ CD25⁻ splenic T cells from PanIN or PDA mice were used as responders after *in vitro* CD3 stimulation. We then added sorted autologous CD4⁺ CD25⁺ T cells and found that they were able to suppress CD3-induced proliferation of responder cells (Fig. 4C). The suppression was dose dependent, underscoring its specificity. In these suppression assays, we identified T_{reg} as CD4⁺ CD25⁺ cells rather than CD4⁺ Foxp3⁺ cells, because staining cells for Foxp3, a transcription factor, requires permeabilizing the cells and consequently killing them.

Because CD25 can also be used as a marker of T-cell activation, we evaluated CD25 expression on non-T_{reg} populations (i.e., CD4⁺ Foxp3⁻ T cells and CD8⁺ T cells) in the pancreas. In contrast to the majority of CD4⁺ Foxp3⁺ T cells from PanIN or PDA pancreata that expressed CD25, <5.5% on average of CD4⁺ Foxp3⁻ T cells were CD25⁺ in these mice (Supplementary Fig. S1A). Among CD8⁺ T cells, <1% of cells expressed CD25 (Supplementary Fig. S1B). These findings confirm the minimal activation status of effector T cells in these pancreatic neoplasms.

To complete the analysis of lymphocyte subtypes, we examined infiltration of CD19⁺ B cells and CD3⁻ CD49b⁺ natural killer cells into the diseased pancreas. Although pancreatic B cells were observed in some animals, there was no statistically significant difference in the percentage of these cells in normal versus PanIN versus PDA mice (data not shown). Natural killer cells were scarce in any pancreatic histology without a statistically significant increase through disease progression (data not shown).

Infiltration of macrophages and MDSC during progression of pancreatic neoplasia. The infiltration of macrophages and MDSC, two cell types implicated in tumor promotion and immunosuppression, was similarly assessed by both flow cytometry and immunohistochemistry (Fig. 5A and B). We found that disease progression from normal histology to PanIN to PDA was accompanied by a progressive infiltration of both macrophages ($P < 0.001$) and MDSC ($P < 0.001$), but the kinetics of the cellular responses differed.

Macrophages were identified as Gr-1⁻ CD11b⁺ cells by flow cytometry, although these cells expressed additional macrophage markers, such as F4/80 and CD68 (Supplementary Fig. S2). Macrophage infiltration began very early in preinvasive disease, and these cells persisted in PDA (Fig. 5C, left). Gr-1⁻ CD11b⁺ macrophages preferentially accumulated around neoplastic ducts in PanIN mice, even including lesions of the lowest grade (Fig. 5B). Macrophages persisted in localizing to neoplastic epithelium in invasive carcinomas but were also evident in surrounding tumor stroma (Fig. 5B). Notably, Gr-1⁻ CD11b⁺ macrophages did not accumulate in the spleen or salivary gland during pancreatic disease progression (Fig. 5C, middle and right).

MDSC infiltrated with delayed kinetics compared with macrophages. They were noted at slightly elevated levels in PanIN lesions but became a prominent component of the leukocytic infiltrate in PDA (Fig. 5D, left). Like macrophages, MDSC were found in both periductal areas and stroma in PDA (Fig. 5B). In contrast to macrophages, however, MDSC also accumulated strikingly in the spleens from PanIN and PDA mice (Fig. 5D, middle). Although splenocytes from control mice included $1.6 \pm 0.4\%$ (mean \pm SE) Gr-1⁺ CD11b⁺ cells, splenocytes from PDA mice included $20.4 \pm$

5.0% of such cells. This was the only leukocyte subset we found that increased as a percentage in the spleens of PDA mice compared with those of normal mice. Notably, Gr-1⁺ CD11b⁺ myeloid cells did not accumulate in other tissues in PanIN or PDA mice, such as the salivary gland, which was examined as a control exocrine gland and which never develops neoplasia in this model (Fig. 5D, right).

Functional analysis of MDSC. To test the suppressive function of MDSCs observed in this model, we did T-cell proliferation assays measuring [³H]thymidine incorporation for quantification. Sorted splenic T cells were stimulated either with the mitogen ConA or with plate-bound CD3 antibody in the presence or absence of irradiated autologous Gr-1⁺ CD11b⁺ cells. The addition of Gr-1⁺ cells inhibited T-cell proliferation in response to either stimulus (Fig. 6A).

Relationship between MDSC and lymphocytic infiltration in pancreas. Although all *Kras*^{G12D} animals consistently developed robust leukocytic infiltrates in the pancreas, we observed variability from animal to animal in the specific cellular composition of the leukocytic infiltrate, particularly with regard to T-cell infiltration. We therefore explored the hypothesis that the variability in T-cell infiltration might not be random, but rather might be influenced by the infiltration of other types of leukocytes. We examined leukocyte subtypes as percentages of the total CD45⁺ infiltrate present within a given PanIN or PDA pancreas.

We found that the presence of MDSC was strongly associated with a lack of T cells in both PanIN and PDA pancreata. This finding was especially striking for CD8⁺ T cells: there was a near mutual exclusion between Gr-1⁺ CD11b⁺ MDSC and CD8⁺ T cells (Fig. 6B). None of the mice had high levels of both Gr-1⁺ CD11b⁺ MDSC and CD8⁺ T cells. This negative association held regardless of the age of the animal or the extent of disease burden. The association between the lack of CD4⁺ T cells and Gr-1⁺ CD11b⁺ MDSC was weaker and without a mutual exclusion as were the associations of CD8⁺ T cells and CD4⁺ T cells with Gr-1⁻ CD11b⁺ macrophages (Fig. 6C).

Discussion

Increasing evidence gleaned from studies in immune-compromised hosts suggests that cellular mechanisms of immunosurveillance influence tumor development (1, 37). These compelling data are nevertheless indirect and do not address questions about the dynamics of the host immune response to a spontaneously developing tumor, particularly events occurring during the preinvasive stages of the disease. Is the immune system able to recognize neoplastic lesions at the earliest signs of dysplasia, or do such lesions remain immunologically ignored until disruption of tissue architecture? To the extent that a clinically evident tumor in an immune-competent host represents a failure of immunosurveillance, when, during the course of disease progression, does this failure manifest? To address these questions, we tracked the evolution of immunosurveillance in a genetically defined mouse model of pancreatic cancer that recapitulates the clinical, histopathologic, and molecular features of human PDA, beginning with its earliest precursor lesions. This model is generated by the pancreatic-specific expression of an endogenous oncogenic *Kras*^{G12D} allele, and mice exhibit preinvasive PanINs as early as 2 weeks, that spontaneously progress to invasive and metastatic PDA. We found that disease progression in *Kras*^{G12D} mice from normal histology to PanIN to invasive PDA was accompanied by a progressive infiltration of CD45⁺ cells, with leukocytes comprising nearly half of all cells in PDA tumors. Leukocytes largely consisted of CD11b⁺ macrophages, which clustered around neoplastic ducts

in preinvasive lesions, including those of lowest grade, and persisted throughout PDA. Although CD4⁺ T cells were evident in PanIN, these cells included a sizable fraction of Foxp3⁺ T_{reg}⁻ Gr-1⁺ CD11b⁺ MDSC were first noted in PanIN lesions and eventually became as prominent as macrophages in PDA. MDSC also disrupted splenic architecture, but not other glandular organs, such as the salivary gland. Moreover, there was no indication of antitumor T-cell activity in early disease: CD8⁺ T cells, thought to be critical mediators of antitumor immunity, were scarce in preinvasive lesions, found in only a subset of advanced cancers, and showed little evidence of activation. To confirm these results, we have recently done similar analyses in an additional mouse model of spontaneous PDA that involves mutation of both *Kras* and p53 targeted to the pancreas. Although disease progresses more rapidly in this second model (median survival is ~5 months; ref. 38), we still found that both the composition and the kinetics of leukocytic infiltration were highly similar to that described here. In particular, we noted a prevalence of macrophages and MDSC in both PanIN and PDA, and a T-cell infiltrate characterized mostly by T_{reg} with a negligible effector response (data not shown). Thus, in contrast to the supposition that early, productive antitumor immune responses are ultimately overwhelmed and bypassed as tumors grow and invade, our data suggest that CD8⁺ T-cell responses encounter multiple, preexisting components of host immunosuppression and are therefore either blunted before immunologic elaboration or never initiated at all.

Of the three major leukocyte subtypes we found in preinvasive lesions, i.e., macrophages, MDSC, and T_{reg}, each has been implicated in mechanisms of tumor promotion or tumor immune suppression. Tumor-associated macrophages have been associated with poor prognosis in many types of cancer, likely due in part to their production of an array of factors that promote angiogenesis and tissue invasion (39). Their presence within tumors has been attributed as a response to hypoxia, where they are presumably recruited to facilitate angiogenesis (40). However, we identified macrophages intimately associated with low-grade neoplastic lesions, unlikely to be a hypoxic microenvironment, and even before evidence of other components of inflammation or stromal remodeling. In our model, which is driven by a constitutively activated *Kras* allele, downstream products of *Kras* signaling may locally recruit macrophages even at the inception of preinvasive disease. Indeed, there is precedent to suppose that *Kras* signaling may be directly responsible for fostering an inflammatory environment within tumors, as activation of the *Kras* pathway can induce production of chemokines, such as CXCL-8, MIP-2, KC, and MCP-1 (41, 42).

MDSC represent a second immunosuppressive myeloid cell type that infiltrates diseased pancreata in this model. These cells also accumulate dramatically in the spleen, but not in other tissues that are unaffected by disease. Previous studies of implanted tumor models have shown that MDSC, identified by the dual expression of Gr-1 and CD11b, are found within the graft microenvironment and can suppress specific T-cell responses *in vitro* (16, 43, 44). The mechanisms by which MDSC exert their suppressive activities are not yet fully understood but involve production of reactive oxygen species in arginase-dependent and inducible nitric oxide synthase-dependent pathways (45). The suppressive properties of these cells are dependent on tumor-derived factors, such as IL-6, IL-10, vascular endothelial growth factor, and granulocyte macrophage colony-stimulating factor (45), and removal of the primary tumor results in a decrease of MDSC and restores T-cell function (46). In implanted tumor models, depleting MDSC seems to augment the

effects of immunotherapy (47, 48). Moreover, MDSC have also been implicated in angiogenesis due to their ability to produce matrix metalloproteinase-9 and to incorporate directly into new tumor vasculature (17). Our findings suggest yet another detrimental function of these cells: we observed a strong inverse correlation between the prevalence of MDSC and CD8⁺ T cells in the leukocytic infiltrate, regardless of the age of the animal or the stage of disease, raising the possibility that MDSC may negatively affect T-cell trafficking or T-cell survival within the neoplasm. The potential antagonism between these two cell types was further underscored by our *in vitro* functional assays, demonstrating that MDSC are capable of suppressing T-cell proliferation.

The third immunosuppressive population that was noted in the early infiltration of PanIN T_{reg} has been intensely scrutinized in recent years for its role in advanced cancer (30, 31). T_{reg} can suppress effector T-cell activation, proliferation, and cytokine production (49). Cell-to-cell contact is required for T_{reg}-mediated suppression, at least *in vitro*, and certain cytokines, such as IL-10 and transforming growth factor- β , have been implicated mechanistically in their function, although these requirements may vary from system to system (49). T_{reg} play a critical physiologic role in guarding against the development of autoimmune disease by preventing activation of autoreactive T cells and curtailing both innate and adaptive immune responses (50). In late-stage cancer patients, however, increased numbers of T_{reg} likely contribute to immune dysfunction, and increased numbers of intratumoral T_{reg} have been associated with reduced survival (51). Here, we show that T_{reg} infiltrate very early in disease progression, at the preinvasive state and before experimental evidence of an adaptive CD8⁺ T-cell response, suggesting that T_{reg} infiltration does not necessarily represent only the contraction phase of an earlier immune response.

Overall, our results show that suppressive cellular elements of the host immune system appear early during pancreatic tumorigenesis, preceding and outweighing antitumor cellular immunity, and likely contribute to disease progression. The resurgent theory of cancer immunosurveillance, however, holds that the immune system can recognize and destroy precursor lesions before they become clinically apparent (1). It has been predicted that if immunosurveillance plays an important role in the suppression of tumors, then early neoplastic lesions should trigger vigorous immune responses (1, 52), such as that observed in patients with premalignant monoclonal gammopathy (53). The "elimination phase" of cancer immunosurveillance is, of course, not always successful, and tumors with reduced immunogenicity or those that have acquired mechanisms to suppress immune effector functions are thought to emerge from this selection pressure and ultimately kill the host (1, 37). Our findings, on the other hand, suggest that at least in a spontaneous model of *in situ* pancreatic cancer in immune-competent animals, the "elimination phase" may be nearly nonexistent. In other words, effector cells of the adaptive immune system may be so sparse or so sufficiently restrained by immunosuppressive leukocytes at even the earliest stages of neoplasia that tumor immune escape is hardly necessary. Thus, the failure of immunosurveillance may be quite an early event during tumorigenesis.

Finally, our results have important clinical implications. In humans, pancreatic cancer is an essentially uniformly fatal disease. Even when fortuitously (and rarely) discovered at resectable stages and despite the combined use of surgery, radiation, chemotherapy, and biologics, 5-year survival is very poor (54). Although immunotherapy holds promise as a novel strategy in human pancreatic cancer (55), our data highlight the potential obstacles posed by mechanisms of immunosuppression derived not only from the

tumor but also from the tumor-associated leukocytic response. Efforts to test potent inhibitors of MDSC, tumor-associated macrophages, and T_{reg} represent important next steps for developing novel immunotherapy of cancer, particularly in combination with state-of-the-art vaccines or adoptive T-cell therapy. However, in light of our data that immunosuppressive factors are operative even at the inception of neoplasia, there is a strong implication that ultimately, active immunotherapy may have to be delivered in a truly preventative setting for it to consistently affect the natural history of cancer.

References

- Smyth MJ, Dunn GP, Schreiber RD. Cancer immunosurveillance and immunoeediting: the roles of immunity in suppressing tumor development and shaping tumor immunogenicity. *Adv Immunol* 2006;90:1–50.
- Van den Eynde BJ, van der Bruggen P. T cell defined tumor antigens. *Curr Opin Immunol* 1997;9:684–93.
- Burnet F. Cancer—a biological approach. *Br Med J* 1957; 1:841–7.
- Dighe AS, Richards E, Old LJ, Schreiber RD. Enhanced *in vivo* growth and resistance to rejection of tumor cells expressing dominant negative IFN γ receptors. *Immunity* 1994;1:447–56.
- van den Broek ME, Kagi D, Ossendorp F, et al. Decreased tumor surveillance in perforin-deficient mice. *J Exp Med* 1996;184:1781–90.
- Kaplan DH, Shankaran V, Dighe AS, et al. Demonstration of an interferon γ -dependent tumor surveillance system in immunocompetent mice. *Proc Natl Acad Sci U S A* 1998;95:7556–61.
- Shankaran V, Ikeda H, Bruce AT, et al. IFN γ and lymphocytes prevent primary tumour development and shape tumour immunogenicity. *Nature* 2001;410: 1107–11.
- Clemente CG, Mihm MC, Jr., Bufalino R, Zurrida S, Collini P, Cascinelli N. Prognostic value of tumor infiltrating lymphocytes in the vertical growth phase of primary cutaneous melanoma. *Cancer* 1996;77: 1303–10.
- Vesalainen S, Lipponen P, Talja M, Syrjänen K. Histological grade, perineural infiltration, tumour-infiltrating lymphocytes and apoptosis as determinants of long-term prognosis in prostatic adenocarcinoma. *Eur J Cancer* 1994;30A:1797–803.
- Marrogi AJ, Munshi A, Merogi AJ, et al. Study of tumor infiltrating lymphocytes and transforming growth factor- β as prognostic factors in breast carcinoma. *Int J Cancer* 1997;74:492–501.
- Naito Y, Saito K, Shiiba K, et al. CD8+ T cells infiltrated within cancer cell nests as a prognostic factor in human colorectal cancer. *Cancer Res* 1998;58:3491–4.
- Zhang L, Conejo-Garcia JR, Katsaros D, et al. Intratumoral T cells, recurrence, and survival in epithelial ovarian cancer. *N Engl J Med* 2003;348:201–11.
- Galon J, Costes A, Sanchez-Cabo F, et al. Type, density, and location of immune cells within human colorectal tumors predict clinical outcome. *Science* 2006;313:1960–4.
- Mantovani A, Schioppa T, Porta C, Allavena P, Sica A. Role of tumor-associated macrophages in tumor progression and invasion. *Cancer Metastasis Rev* 2006; 25:315–22.
- Almand B, Clark JI, Nikitina E, et al. Increased production of immature myeloid cells in cancer patients: a mechanism of immunosuppression in cancer. *J Immunol* 2001;166:678–89.
- Gabrilovich DI, Velders MP, Sotomayor EM, Kast WM. Mechanism of immune dysfunction in cancer mediated by immature Gr-1+ myeloid cells. *J Immunol* 2001;166:5398–406.
- Yang L, DeBusk LM, Fukuda K, et al. Expansion of myeloid immune suppressor Gr-1+CD11b+ cells in tumor-bearing host directly promotes tumor angiogenesis. *Cancer Cell* 2004;6:409–21.
- Kusmartsev S, Gabrilovich DI. Role of immature myeloid cells in mechanisms of immune evasion in cancer. *Cancer Immunol Immunother* 2006;55:237–45.
- de Visser KE, Korets LV, Coussens LM. *De novo* carcinogenesis promoted by chronic inflammation is B lymphocyte dependent. *Cancer Cell* 2005;7:411–23.
- Onizuka S, Tawara I, Shimizu J, Sakaguchi S, Fujita T, Nakayama E. Tumor rejection by *in vivo* administration of anti-CD25 (interleukin-2 receptor α) monoclonal antibody. *Cancer Res* 1999;59:3128–33.
- Shimizu J, Yamazaki S, Sakaguchi S. Induction of tumor immunity by removing CD25+CD4+ T cells: a common basis between tumor immunity and autoimmunity. *J Immunol* 1999;163:5211–8.
- Garside P, Ingulli E, Merica RR, Johnson JG, Noelle RJ, Jenkins MK. Visualization of specific B and T lymphocyte interactions in the lymph node. *Science* 1998;281: 96–9.
- Okada T, Cyster JG. B cell migration and interactions in the early phase of antibody responses. *Curr Opin Immunol* 2006;18:278–85.
- Hingorani SR, Petricoin EF, Maitra A, et al. Preinvasive and invasive ductal pancreatic cancer and its early detection in the mouse. *Cancer Cell* 2003;4:437–50.
- Leach SD. Mouse models of pancreatic cancer: the fur is finally flying! *Cancer Cell* 2004;5:7–11.
- Hruban RH, Goggins M, Parsons J, Kern SE. Progression model for pancreatic cancer. *Clin Cancer Res* 2000;6:2969–72.
- Tuveson DA, Hingorani SR. Ductal pancreatic cancer in humans and mice. *Cold Spring Harb Symp Quant Biol* 2005;70:65–72.
- Hruban RH, Adsay NV, Albores-Saavedra J, et al. Pathology of genetically engineered mouse models of pancreatic exocrine cancer: consensus report and recommendations. *Cancer Res* 2006;66:95–106.
- Dutton RW, Bradley LM, Swain SL. T cell memory. *Annu Rev Immunol* 1998;16:201–23.
- Sakaguchi S, Sakaguchi N, Shimizu J, et al. Immunologic tolerance maintained by CD25+ CD4+ regulatory T cells: their common role in controlling autoimmunity, tumor immunity, and transplantation tolerance. *Immunol Rev* 2001;182:18–32.
- Shevach EM. CD4+ CD25+ suppressor T cells: more questions than answers. *Nat Rev Immunol* 2002;2:389–400.
- Fontenot JD, Gavin MA, Rudensky AY. Foxp3 programs the development and function of CD4+CD25+ regulatory T cells. *Nat Immunol* 2003;4:330–6.
- Fontenot JD, Rasmussen JP, Williams LM, Dooley JL, Farr AG, Rudensky AY. Regulatory T cell lineage specification by the forkhead transcription factor foxp3. *Immunity* 2005;22:329–41.
- Hori S, Nomura T, Sakaguchi S. Control of regulatory T cell development by the transcription factor Foxp3. *Science* 2003;299:1057–61.
- Sakaguchi S, Sakaguchi N, Asano M, Itoh M, Toda M. Immunologic self-tolerance maintained by activated T cells expressing IL-2 receptor α -chains (CD25). Breakdown of a single mechanism of self-tolerance causes various autoimmune diseases. *J Immunol* 1995; 155:1151–64.
- Sakaguchi S. Naturally arising Foxp3-expressing CD25+CD4+ regulatory T cells in immunological tolerance to self and non-self. *Nat Immunol* 2005;6:345–52.
- Dunn GP, Old LJ, Schreiber RD. The three Es of cancer immunoeediting. *Annu Rev Immunol* 2004;22: 329–60.
- Hingorani SR, Wang L, Multani AS, et al. Trp53R172H and KrasG12D cooperate to promote chromosomal instability and widely metastatic pancreatic ductal adenocarcinoma in mice. *Cancer Cell* 2005;7:469–83.
- Pollard JW. Tumour-educated macrophages promote tumour progression and metastasis. *Nat Rev Cancer* 2004;4:71–8.
- Knowles H, Leek R, Harris AL. Macrophage infiltration and angiogenesis in human malignancy. *Novartis Found Symp* 2004;256:189–200.
- Sparmann A, Bar-Sagi D. Ras-induced interleukin-8 expression plays a critical role in tumor growth and angiogenesis. *Cancer Cell* 2004;6:447–58.
- Ji H, Houghton AM, Mariani TJ, et al. K-ras activation generates an inflammatory response in lung tumors. *Oncogene* 2006;25:2105–12.
- Bronte V, Wang M, Overwijk WW, et al. Apoptotic death of CD8+ T lymphocytes after immunization: induction of a suppressive population of Mac-1+/Gr-1+ cells. *J Immunol* 1998;161:5313–20.
- Kusmartsev SA, Li Y, Chen SH. Gr-1+ myeloid cells derived from tumor-bearing mice inhibit primary T cell activation induced through CD3/CD28 costimulation. *J Immunol* 2000;165:779–85.
- Serafini P, Borrello I, Bronte V. Myeloid suppressor cells in cancer: recruitment, phenotype, properties, and mechanisms of immune suppression. *Semin Cancer Biol* 2006;16:53–65.
- Salvadori S, Martinelli G, Zier K. Resection of solid tumors reverses T cell defects and restores protective immunity. *J Immunol* 2000;164:2214–20.
- Kusmartsev S, Cheng F, Yu B, et al. All-trans-retinoic acid eliminates immature myeloid cells from tumor-bearing mice and improves the effect of vaccination. *Cancer Res* 2003;63:4441–9.
- Suzuki E, Kapoor V, Jassar AS, Kaiser LR, Albelda SM. Gemcitabine selectively eliminates splenic Gr-1+/CD11b+ myeloid suppressor cells in tumor-bearing animals and enhances antitumor immune activity. *Clin Cancer Res* 2005;11:6713–21.
- Miyara M, Sakaguchi S. Natural regulatory T cells: mechanisms of suppression. *Trends Mol Med* 2007;13: 108–16.
- Wing K, Fehervari Z, Sakaguchi S. Emerging possibilities in the development and function of regulatory T cells. *Int Immunol* 2006;18:991–1000.
- Curiel TJ, Coukos G, Zou L, et al. Specific recruitment of regulatory T cells in ovarian carcinoma fosters immune privilege and predicts reduced survival. *Nat Med* 2004;10: 942–9.
- Zitvogel L, Tesniere A, Kroemer G. Cancer despite immunosurveillance: immunoselection and immunosubversion. *Nat Rev Immunol* 2006;6:715–27.
- Dhodapkar MV, Krasovskiy J, Osman K, Geller MD. Vigorous premetastatic-specific effector T cell response in the bone marrow of patients with monoclonal gammopathy. *J Exp Med* 2003;198:1753–7.
- Jemal A, Siegel R, Ward E, et al. Cancer statistics, 2006. *CA Cancer J Clin* 2006;56:106–30.
- LaHeru D, Jaffee EM. Immunotherapy for pancreatic cancer - science driving clinical progress. *Nat Rev Cancer* 2005;5:459–67.